Int. J. Electrochem. Sci., 5 **(2010)** 1342 - 1354

International Journal of
ELECTROCHEMICAL
SCIENCE
www.electrochemsci.org

Electrocatalytic Performance of In_2O_3-Supported Pt/C Nanoparticles for Ethanol Electro-oxidation in Direct Ethanol Fuel Cells

Javier Parrondo[1], *R. Santhanam*[1], *Federico Mijangos*[2], *B. Rambabu*[1,*]

[1] Solid State Ionics and Surface Sciences Lab, Department of Physics,
Southern University and A&M College, Baton Rouge, LA 70813, USA
[2] Department of Chemical Engineering, University of the Basque Country,
Bilbao, Vizcaya 48940, Spain
[*]E-mail: rambabu@cox.net

Received: 19 July 2010 / *Accepted:* 30 July 2010 / *Published:* 1 September 2010

In_2O_3 supported Pt/C (Pt/C- In_2O_3) composite electrocatalysts has been prepared from In_2O_3 nanoparticles prepared by chemical reduction process and the commercially available Pt/C. X-ray diffraction, scanning electron microscopy-energy dispersive spectroscopy (SEM-EDS) show that In_2O_3 nanoparticles are well distributed on Pt/C and In_2O_3 has the crystallite size of 20 nm. High resolution transmission electron microscopy (HR-TEM) also indicates that the In_2O_3 particles with a crystallite size of 5 nm are highly dispersed on the surface of the Pt/C. The Pt/C- In_2O_3 nanoparticles demonstrate a higher activity towards ethanol oxidation than Pt/C despite lower electrochemical surface area. Since Nafion membrane is not suitable for high operating temperature, the experiments are conducted using phosphoric acid doped polybenzimidazole (PBI) membrane. Fuel cell polarization data are obtained using Pt/C and Pt/C-In_2O_3 at different high operating temperatures with oxygen as oxidant and ethanol as fuel. In all the test conditions, the performance of Pt/C-In_2O_3 is found to be higher compared to that of Pt/C. This result indicates the active participation of In_2O_3 significantly improves the catalytic activity of Pt/C in the ethanol oxidation process. Hence, these results suggest that In_2O_3 supported Pt/C assembled with PBI membrane could be considered as an effective composite electrocatalyst for ethanol oxidation at high temperature in direct ethanol fuel cells.

Keywords: electrocatalysis; ethanol fuel cell; In_2O_3; Pt nano particles

1. INTRODUCTION

Direct alcohol fuel cells (DAFCs) have attracted much attention as advanced power sources of energy for a variety of applications, for portable electronic devices and fuel cell vehicles [1-5]. Among various liquid fuels, methanol has been extensively examined as a primary fuel for DAFC because of its low cost, easy storage, wide availability and low green house gases emission [6-9]. However, use of ethanol as a fuel in DAFCs provides several advantages over methanol due to its low toxicity, safety, renewability, high energy density and easy production in large quatities from agricultural products [10-13]. Until now, Pt and Pt-based catalysts are considered to be the most promising electrode materials for DAFCs. They have been extensively studied as electrocatalysts for electro-oxidation of methanol and ethanol [14-17]. However, it is well-known that Pt is very costly and its supply is limited which constitute a major barrier for the development of DAFCs.

Another key issue inhabiting its commercialization is the low alcohol electro-oxidation kinetics caused by catalyst poisoning. Therefore, it is indeed a need to develop catalysts with low Pt loading or Pt free catalysts.

Conventionally, carbon materials are used as supports for Pt and Pt-based alloy catalysts in both anodes and cathodes of DAFCs and proton exchange membrane fuel cells (PEMFCs) to minimize the use of precious metal [18-20]. Since carbon nano tubes (CNTs) have unique structural and electrical properties, they have been investigated as catalyst supports for applications in fuel cells by different research groups [21-23]. However, carbon materials have weak interaction with the nanoparticles of the catalysts and also they do not help to improve electrocatalytic activities. Carbon is known to oxidize to CO_2 in aqueous solutions and Pt further increases the corrosion rate of carbon which in turn leads to severe agglomeration and growth of catalyst particles and this results degradation in the fuel cell performance [24].

Recently, Pt-based catalysts decorated with oxides such as TiO_2, SnO_2, CeO_2, RuO_2, ZrO_2 etc have been intensively studied to understand the improvement on the catalytic activity and stability for the electro-oxidation reactions of ethanol [25-29]. It has been found that the oxide materials have much higher corrosion resistance and smaller decrease in the electrochemical active surface area when compared to that of carbon support [30, 31].

Indium oxide (In_2O_3), which is well-known for its excellent gas sensing properties [32, 33] and this material has been widely used to improve the catalytic performance for the steam reforming of methanol and dehydrogenation of ethanol [34, 35].

Chu et al. studied the electrochemical activity of ethanol oxidation using the Pd-In_2O_3/CNTs composite catalyst in alkaline solutions [36]. They found that the Pd-In_2O_3/CNTs electrocatalyst exhibited higher activity for ethanol oxidation than Pd/CNTs. Park et al. studied the electrocatalytic properties of indium tin oxide (ITO) supported Pt nanoparticles for methanol electro-oxidation and they explained that the high catalytic activity of ITO supported Pt is related to the active participation of ITO in the methanol oxidation process [37]. In the present work, unlike previous work related to In_2O_3 for DAFCs, we present the preparation and catalytic activities of Pt/In_2O_3/C composite catalysts with different compositions of In_2O_3 as anode catalyst for polybenzimazole (PBI)-based high temperature-direct ethanol fuel cells (HT-DEFCs).

Fuel cell performance measurements are carried out in the temperature range between 160 and 200^oC to determine the stability and feasibility of the Pt/In_2O_3/C composite catalysts for HT-DEFCs.

2. MATERIAL AND METHODS

Platinum supported over In_2O_3 and Carbon was prepared by mixing the appropriate amounts of 40% Pt/C (Alfa Aesar) and nanosized Indium oxide (In_2O_3). In_2O_3 was prepared by using indium nitrate (Alfa Aesar) and hexamethylenetetramine (HMT 99%, Alfa Aesar) as the starting materials. A stock solution (0.5 mol L^{-1}) of HMT in deionized water was prepared and added drop wise to a stock solution (0.04 mol L^{-1}, pH 1) of indium (III) nitrate. The HMT would slowly hydrolyze to yield ammonia and formaldehyde. Then, the solution was stirred at room temperature overnight to allow complete precipitation of the hydroxide. After that, the precipitate was recovered by centrifuge, washed twice with isopropanol and dry overnight at room temperature. To obtain indium oxide, the hydroxide thus obtained was heated at 400 °C for 2 hours.

m-PBI was synthesized following the procedure described by Xiao et al. [38, 39]. In a typical synthesis, 3.7135 g of isophthalic acid (22.35 mmol) and 4.7896 g of 3, 3'-diaminobenzidine (22.35 mmol) were added to a three-neck reaction flask in an Argon filled Glovebox, followed by 91.5 g of polyphosphoric acid. The reaction mixture was stirred using a mechanical overhead stirrer and purged with a slow stream of nitrogen and maintained at 200 °C during 24 h. The membranes were prepared by casting the polyphosphoric acid (PPA) polymer solution onto glass plates using an adjustable film applicator (GARDCO MICROM II, Paul N. Gardner Company). The gate clearance was fixed in 0.015 cm to obtain membranes of approximately 100 μm after hydrolysis. The acid content of the PBI membrane was 85 wt.%. PBI solution (5 wt.%) in N,N-dimethylacetamide was prepared with the aid of lithium chloride (1.5 wt.%) in an autoclave at 250°C and 6.3 bar for 6 h. The homogeneous solution obtained was subsequently used to prepare catalyst ink [40].

Gas Diffusion Electrodes (GDEs) were prepared by painting using an airbrush over the microporous area of commercial gas diffusion layer (GDL Sigracet GDL 10BB, 420 μm, SGL Carbon Group). Catalyst ink consisted of 0.2 g of catalyst to which 7.5 g of DMAc and 0.21 g of 5 wt.% PBI solution were added. The ink slurry was stirred overnight to break up the catalyst powder in order to get a homogenous ink. During painting, the GDL was kept near a lamp to dry the ink between each application. The Pt loading of each electrode was measured by the difference in weight before and after painting and was kept in 1.40 ±0.05 mg cm^{-2} for the cathode and 2.40 ±0.05 mg cm^{-2} for the anode. Platinum nominally 40% on carbon black (Alfa Aesar) was used for the preparation of the cathodes.

Cyclic voltammograms (CV) were obtained with a conventional three-electrode electrochemical cell using a glassy carbon electrode (1.5 mm diameter) as a working electrode, Pt wire as a counter electrode, and Ag/AgCl (3.5 M KCl) as a reference electrode. Electrochemical data were collected with a Princeton Applied Research Potentiostat/Galvanostat model 273A and are reported vs normal hydrogen electrode (NHE). The glassy carbon electrode was polished with 10 nm silica. For the preparation of the ink slurry, 2 g of deionized water and 0.05 g of catalyst were mixed and sonicated until the ink slurry became homogeneous. 10 μL of the ink slurry was dropped onto the glassy carbon electrode with a micropipette and allowed to dry. After dried, 5 μL of 5% Nafion solution (Ion Power) was placed over the electrode and allowed to dry. The CV plots were recorded in the potential range of 0.05–1.2 V vs NHE with a scan rate of 50 mV/s after purging the 0.5 M H_2SO_4

or 0.5 M H_2SO_4 + 1 M ethanol solution with nitrogen gas for 30 min. To assure reproducibility the electrodes were prepared and tested five times.

The performance of the MEAs was evaluated by using a Compact Fuel Cell Test System model 850e (Scribner Associates, Inc.) controlled using FuelCell® 3.9c software. The polarization curves were recorded at atmospheric pressure using dry oxygen (0.1 L/min) and ethanol solution (1 mL/min) at temperatures ranging from 160 to 200 °C. The ethanol was introduced in the DEFC using a Gilson (Model Miniplus 3) peristaltic pump controlled using Fuel Cell®. The liquid fuel was vaporized before entering the cell flow fields using the build-in pre-heater of the DMFC hardware.MEAs with an active area of 3.24cm^2 were assembled by placing two gas diffusion electrodes (GDEs) on both sides of the PBI membrane in a 5cm^2 single cell DMFC with single serpentine flow fields (Fuel Cell Technologies, Inc.), using sub-gaskets to avoid direct pressure of the gaskets over the membrane and hence protecting the membrane from excessive pressure and stress during heating. The sub-gaskets had a thickness of 25μm and the gaskets 395μm. The pinch, defined as the difference between thickness of the MEA and the gaskets, was 75μm.

3. RESULTS AND DISCUSSION

The synthesized Pt/C, In_2O_3, and Pt/C/In_2O_3 electrocatalysts were analyzed by X-ray diffraction (XRD) measurements and the XRD patterns of these catalysts are shown in Fig. 1.

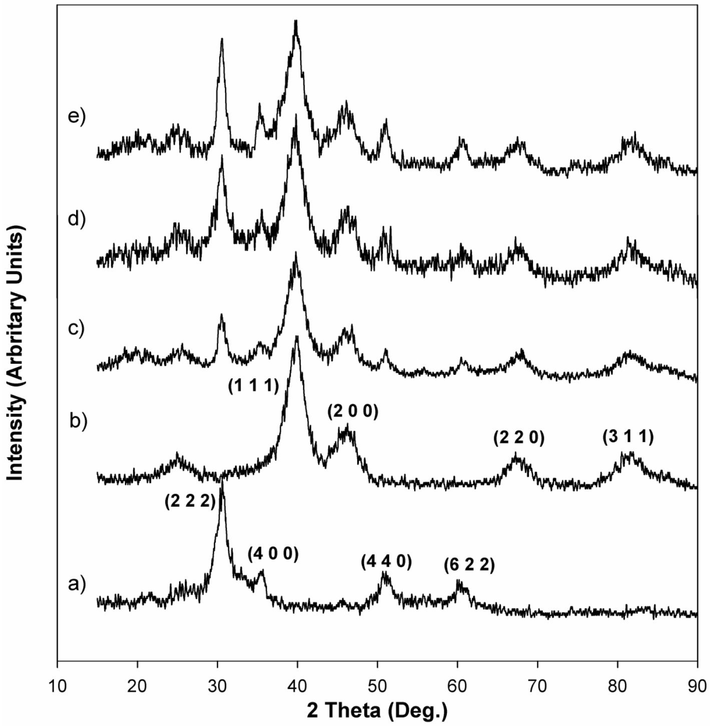

Figure 1. X-ray diffraction patterns of (a)In_2O_3, (b) Pt/C, (c) 90%Pt/C-10%In_2O_3, (d)80%Pt/C-20% In_2O_3 and (e) 60%Pt/C-40% In_2O_3.

As seen in Fig. 1b, the XRD pattern of Pt/C shows characteristic peaks at the Bragg angles of 40°, 47°, 68°, 81° correspond to the (1 1 1), (2 0 0), (2 2 0) and (3 1 1) planes of face-centered cubic structure of Pt (JCPDS card number 87-0640). The peak at around 25° should be attributed to the hexagonal structure of carbon support. It is clear from Fig. 1a that the diffraction pattern of In_2O_3 nanoparticles at the Bragg angles of 31°, 36°, 51°, 60° correspond to the (2 2 2), (4 0 0), (4 4 0) and (6 2 2) planes of the bulk cubic structure of In_2O_3 (JCPDS card number 6-0416). Diffraction patterns for Pt/C-In_2O_3 electrocatalysts showed the diffraction peaks from both Pt particles and In_2O_3. As In_2O_3 loading increased, the diffraction peaks of the In_2O_3 increased correspondingly, especially the peak corresponds to (2 2 2) plane of In_2O_3.

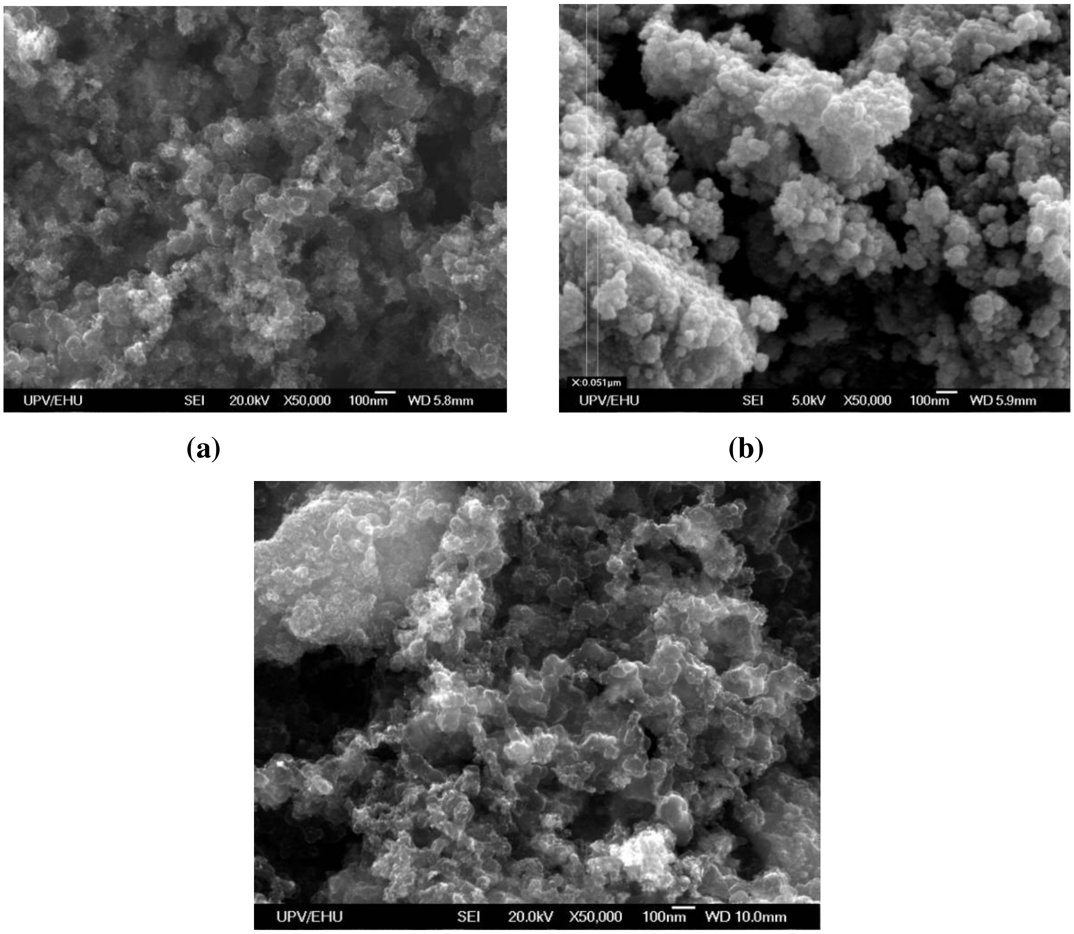

(a) **(b)**

(c)

Figure 2. SEM images of (a) Pt/C, (b) In_2O_3 and (c) Pt/C-In_2O_3.

Microscopic measurements were carried out to provide information on the morphology, particle size and particle size distribution of Pt/C and In_2O_3. Scanning electron microscopy (SEM) images of Pt/C, In_2O_3 and Pt/C-In_2O_3 (60:40) catalysts are shown in Fig. 2a-c, respectively. Pt particles are uniformly distributed on the carbon support as seen in Fig. 2a (Pt distribution is more clear in TEM images). In_2O_3 particles are agglomerated and are seen as bright big particles (Fig. 2b). The presence of agglomerated In_2O_3 particles is clearly seen with Pt/C in Fig. 2c. Fig. 3 shows a representative SEM image and the corresponding EDS spectrum of the as-prepared Pt/C-In_2O_3 electrocatalyst. The EDS spectrum obtained at different locations reveal the presence of In, Pt and C elements in the Pt/C-In_2O_3 electrocatalyst (Fig. 3b-d). Spectrum 1 & 2 were taken at bright locations and spectrum 3 was taken from dark location. From the EDS results, it can be suggested that the bright spots are In_2O_3 (intensity of In peak is higher than Pt peak in spectrum 1&2) and the dark area indicates the distribution of Pt particles on carbon support (Pt peak intensity is higher than in spectrum 3).

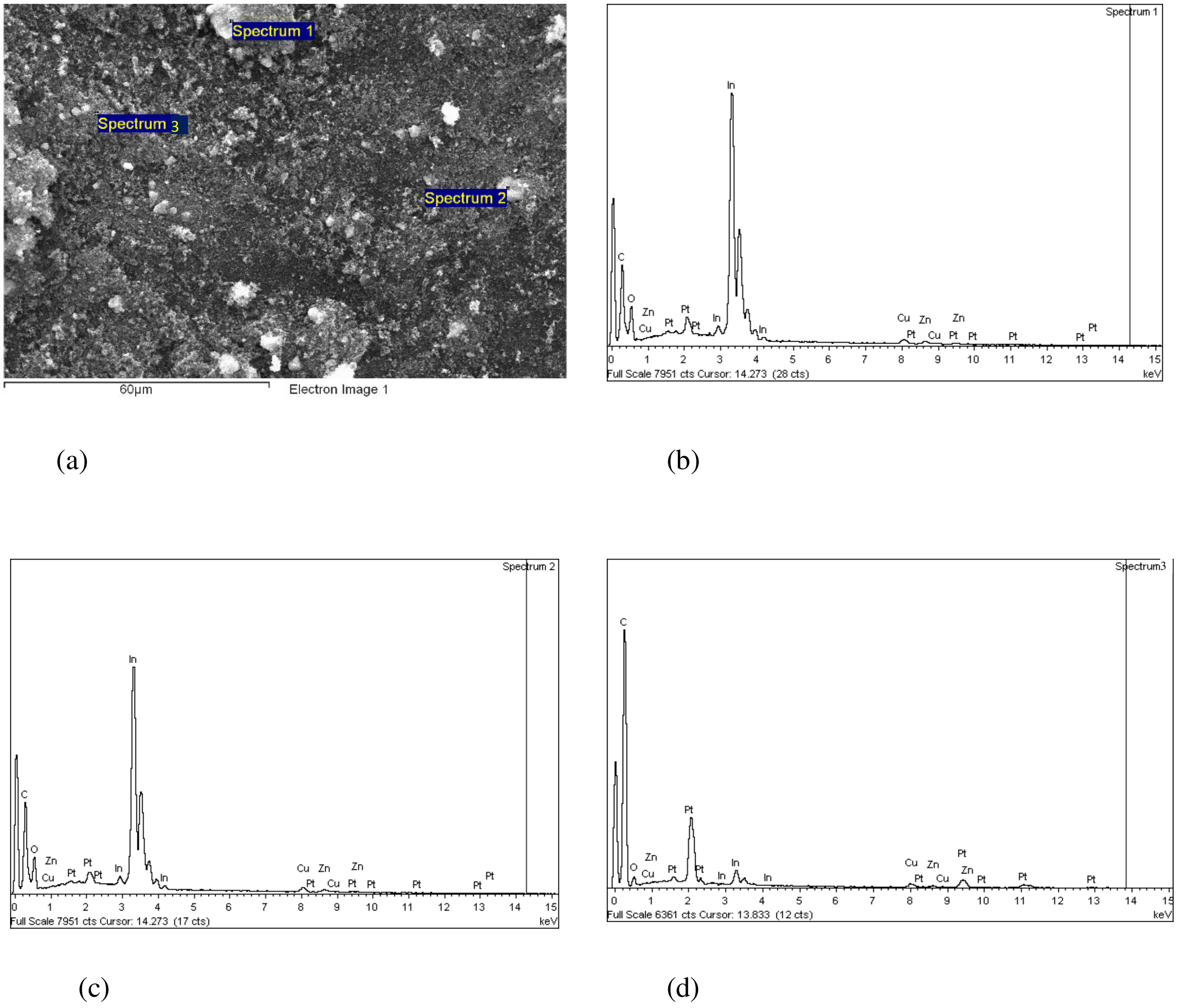

Figure 3. SEM image of Pt/C-In_2O_3 and the EDX spectrum obtained at different locations on the image.

Transmission electron microscopy (TEM) images were obtained to provide more information on particle size and distribution. Fig. 4a-4c shows the TEM images of Pt/C, In_2O_3 and Pt/C-In_2O_3 particles, respectively. As seen in Fig. 4a, the Pt particles are uniform and well-distributed. The average particle size from TEM images was 5 nm. The TEM image of In_2O_3 shows that the particles are agglomerated as shown in Fig. 4b. As can be seen clearly in the TEM image of Pt/C-In_2O_3 (Fig. 4c), the Pt nanoparticles and the agglomerated In_2O_3 particles are distributed uniformly on the carbon support.

Cyclic voltammograms of Pt/C and Pt/C-In_2O_3 (different ratio) electrocatalysts in 0.5M H_2SO_4 are shown in Fig. 5. All of them showed H-adsorption/desorption peaks and Pt-oxide formation/reduction peaks. The anodic peaks appeared around 0.55V indicates the oxidation of In-O species (not seen for Pt/C sample) and the peak current increased with increasing In_2O_3 content. As seen in Fig. 5, Pt/C-In_2O_3 samples show the well-defined Pt properties in the hydrogen and oxygen regions similar to that of Pt/C sample. The electrochemical surface areas (ESA) calculated using hydrogen desorption peak and area specific current densities of the as-prepared electrocatalysts are compiled in Table 1.

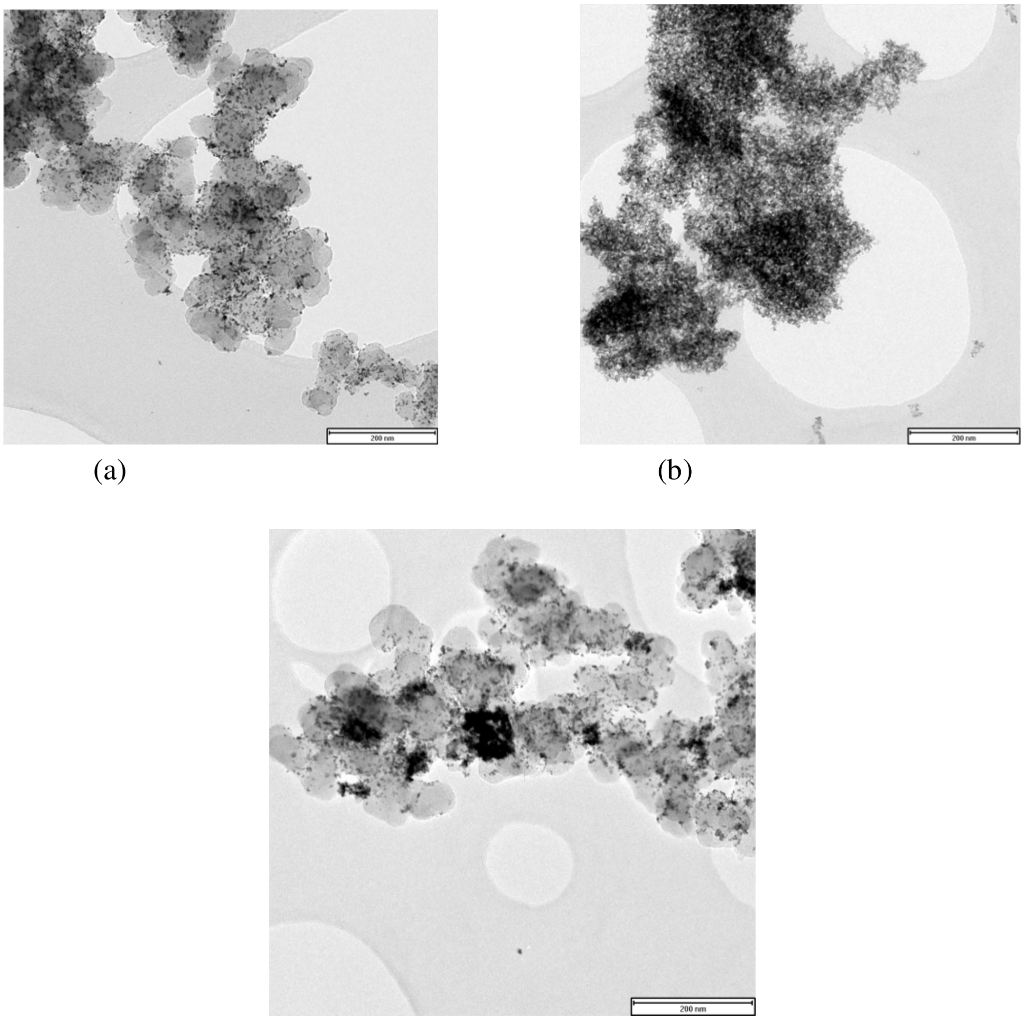

(a) (b)

(c)

Figure 4. TEM images of (a) Pt/C, (b) In_2O_3 and (c) Pt/C-In_2O_3.

The In_2O_3 supported Pt/C catalysts exhibit electrochemical surface areas lower than that of Pt/C catalyst, however the area specific current density of the In_2O_3 supported Pt/C catalysts increase with decreasing Pt metal loading. For example, ESA of the Pt/C is 3 times higher than 60%Pt/C-40%In_2O_3, but the area specific current density of 60%Pt/C-40%In_2O_3 is 2 times higher than Pt/C which might be due to enhancement of Pt activity by the addition of In_2O_3.

The as-prepared Pt/C and Pt/C-In_2O_3 electrocatalyts were tested for their electrocatalytic activity in the oxidation of ethanol. The electrocatalytic activities of these catalysts were obtained by the cyclic voltammograms recorded in a solution of 0.5M H_2SO_4 + 1M CH_3CH_2OH and are shown in Fig. 6. As can be seen in Fig. 6 and Table 1, the area specific current density of the In_2O_3 supported catalysts increases with decreasing Pt content. Despite the lower electrochemical surface area, Pt/C-In_2O_3 samples show higher area specific current densities than Pt/C sample. This might be mostly due to the enhancement of surface specific activity of the In_2O_3 supported catalysts which in turn may be related to the greater CO tolerance. All the In_2O_3 supported Pt/C catalysts show a higher area specific current density than Pt/C catalyst. The catalytic activity of 60%Pt/C-40%In_2O_3 is approximately 2.5 times higher than that of Pt/C for ethanol oxidation. In addition, the threshold potentials of Pt/C-In_2O_3 electrocatalysts are slightly lower when compared to that of Pt/C catalyst. This result indicates that the In_2O_3 supported Pt/C electrocatalysts have higher catalytic activity at lower potentials than Pt/C catalyst due to addition of In_2O_3.

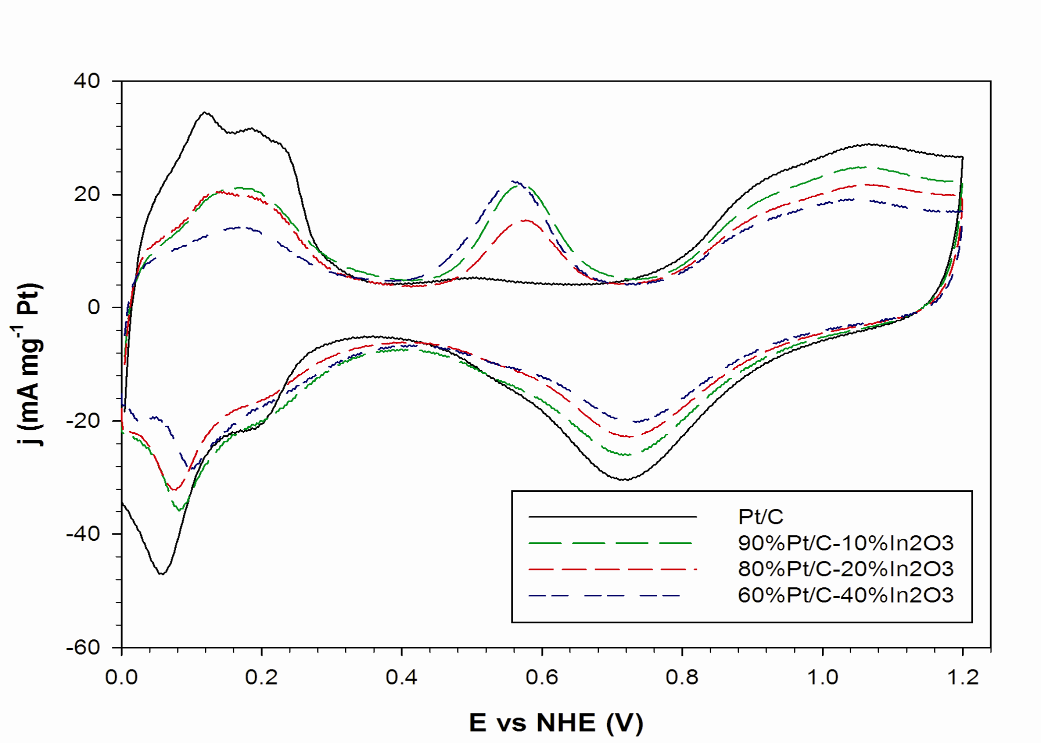

Figure 5. Comparison of the cyclic voltammetry curves of the Pt/C-In_2O_3 catalysts in 0.5 M H_2SO_4 solution.

Table 1. Electrochemical properties of Pt/In_2O_3/C and carbon-supported Pt catalysts.

Catalyst	Electrochemical surface area (m^2/g Pt)	Area-specific current density at 0.6 V (mA/m^2 Pt)*
Pt/C	55.3	154
90%Pt/C-10%In_2O_3	31.9	246
80%Pt/C-20%In_2O_3	30.9	258
60%Pt/C-40%In_2O_3	17.5	323

* in 0.5 M H_2SO_4 + 1 M ethanol

One of the main evaluation parameters for fuel cells is the cell performance. Polarization curves for 60%Pt/C-40%In_2O_3 anode catalyst were recorded at a temperature of 180°C with increasing ethanol concentrations, using oxygen as oxidant with a flow rate of 0.2 L/min. Pure oxygen was used instead of air to exclude potential effects of mass-transport limitations in the cathode side and to get more insight in to the process taking place at the anode side where the electrochemical oxidation of ethanol occurs. As can be seen in Figure 7, the increase of the concentration of ethanol in the feed decreases the performance as well as open circuit voltages (OCVs). This is due to the increase of ethanol crossover at higher concentration that leads to lower voltage as a result of mixed potentials. OCV at 180 ºC decreases from 0.66 V to 0.62 V when the concentration of ethanol in the feed was increased from 3 M to 10 M. The voltage at 1000 mA/m^2 decreases around 100 mV when feeding 10 M ethanol instead of 3 M. From the results obtained in this work, best results are obtained when feeding 3 M ethanol in to the fuel cell.

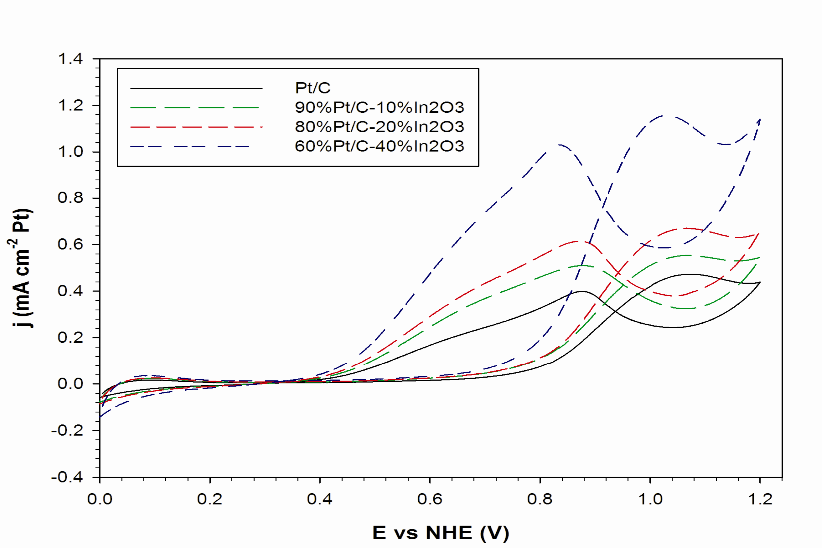

Figure 6. Comparison of area-specific current density of the Pt/C-In_2O_3 catalysts in 0.5 M H_2SO_4 and 1 M ethanol solution.

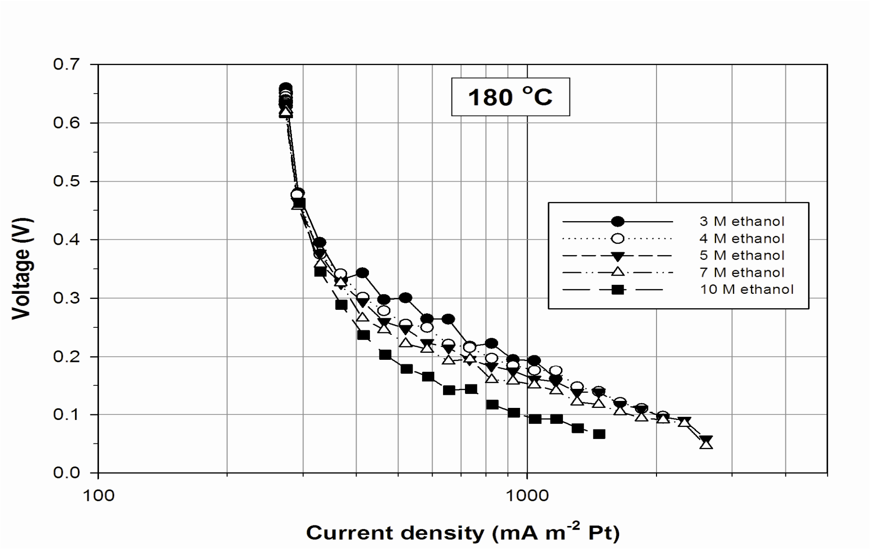

Figure 7. Effect of the concentration of ethanol on the performance of DEFC at 180 °C using 60%Pt/C-40%In_2O_3 catalyst at the anode. Oxygen: 0.1 L/min; fuel: 1 mL/min; cathode Pt loading: 1.4mg cm^{-2}; anode Pt loading: 2.4 mg cm^{-2}.

The effect of the working temperature on the performance of the fuel cell was studied by using 60%Pt/C-40%In_2O_3 catalyst and 3M ethanol solution. The results are shown in Fig. 8. The results show a slight increase in the performance when the temperature was rose which is in good agreement with previously published work [37]. The increase in the electrolyte conductivity with the temperature, along with the enhancement in the kinetics of the electrode reactions, especially for the ethanol oxidation, account for this trend. The voltage increases about 50 mV at 1000 mA/m^2 when the temperature is increased from 160 ºC to 200 ºC.

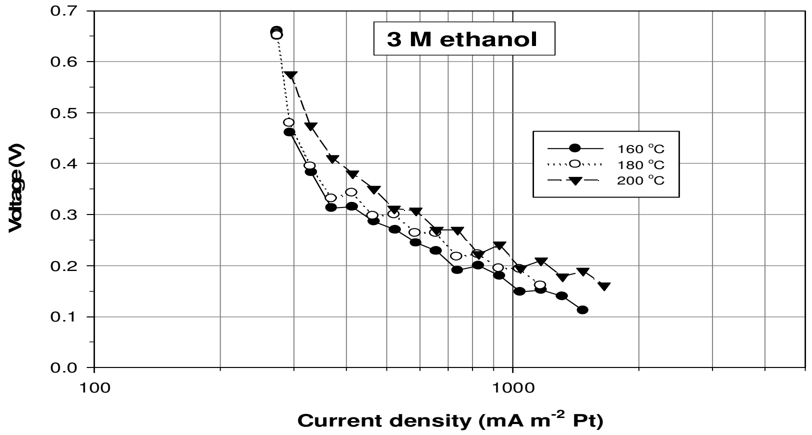

Figure 8. Effect of the temperature on the performance of DEFC using 60%Pt/C-40%In_2O_3 catalyst at the anode. Oxygen: 0.1 L/min; fuel: 1 mL/min; cathode Pt loading: 1.4mg cm^{-2}; anode Pt loading: 2.4 mg cm^{-2}.

The fuel performances obtained from 60%Pt/C-40%In_2O_3 and commercial Pt/C catalysts in the high temperature ethanol fuel cell are presented in Fig. 9. As seen clearly in this figure, a significant improvement is observed in the performance of the fuel cell at low current densities when In_2O_3 supported catalysts is used as anode. For example, at 500 mA/m^2, there is an increase of nearly 100 mV in the output of the fuel cell.

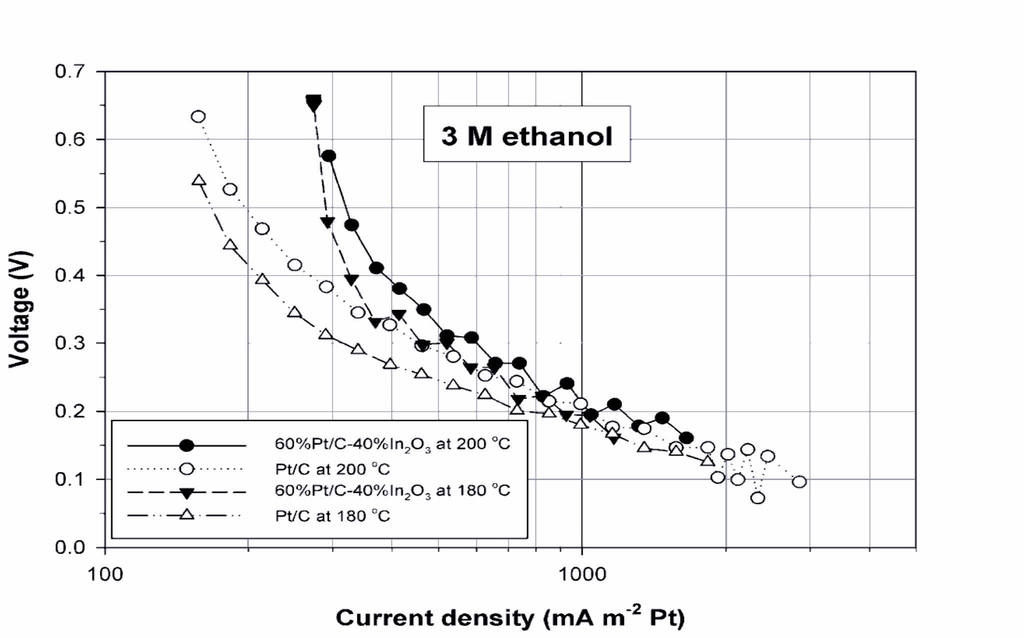

Figure 9. Comparison of performance of DEFC (3M ethanol) with 60%Pt/C-40%In_2O_3 and commercial Pt/C catalysts at different temperatures.

4. CONCLUSIONS

In this work, Pt/C-In_2O_3 composite electrocatalysts were prepared from In_2O_3 nanoparticles, prepared in our laboratory by chemical process, and commercially available Pt/C. Surface characterization data indicate that In_2O_3 (5 nm) was uniformly dispersed on the Pt/C support. The activity of the composite catalysts for ethanol oxidation was investigated by cyclic voltammetry in acidic media. Polarization measurements were carried out by assembling fuel cell using oxygen as an oxidant and ethanol as fuel; the anode materials were tested in a high temperature PEMFC assembled using phosphoric acid doped PBI membrane. Although the In_2O_3 supported Pt/C nanoparticles have lower electrochemical surface area than Pt/C, they exhibit a higher catalytic activity for ethanol electro-oxidation. Fuel cell polarization data demonstrate that the performance of Pt/C-In_2O_3 is found to be higher compared to that of Pt/C at different high operating temperatures. The results evidence that In_2O_3 supported Pt/C could be used as an effective electrocatalyst for ethanol oxidation in direct ethanol fuel cells.

ACKNOWLEDGEMENTS
This work is supported by U.S-DOD-ARO under the grant # W911NF-08-C-0415. BRB and Javier Parrondo thank Dr. Robert Mantz (Electrochemistry and Advanced Energy Conversion) at ARO-Chemical Sciences, and Dr. Thomas L. Reitz (Electrochemistry and Thermal Sciences at AFRL, Wright Patterson Airbase, OH) for supporting fuel cell research at SUBR.

References

1. R. Dillon, S. Srinivasan, A.S. Arico, V. Antonucci*, J. Power Sources* 127 (2004) 112-126.
2. C.K. Dyer, *J. Power Sources* 106 (2002) 31-34.
3. A. O. Neto, R. W. R. Verjulio-Silva, M. Linardi, E.V. Spinace, *Int. J. Electrochem. Sci.* 4 (2009) 954 – 961.
4. J. Arun kumar, P. Kalyani, R. Saravanan, *Int. J. Electrochem. Sci. 3* (2008) 961 – 969.
5. B. Krishnamurthy, S. Deepalochani, *Int. J. Electrochem. Sci.,* 4 (2009) 386 – 395.
6. R.F. Service, *Science* 296 (2002) 1222-1224.
7. G.S. Chai, S.B. Yoon, J.-S. Yu, J.-H. Choi, Y.-E. Sung, *J. Phys. Chem*. B 108 (2004) 7074-7079.
8. Z.B. Wang, G.P. Yin, P.F. Shi, *Carbon* 44 (2005) 133-140.
9. T. Yamaguchi, H. Kuroki, F. Miyata, *Electrochem. Commun*. 7 (2005) 730-734.
10. S. Q. Song, P. Tsiakaras, *Appl. Catal*. B 63 (2006) 187-193.
11. J. Wang, S. Wasmus, R.F. Savinell, *J Electrochem Soc* 142 (1995) 4218-4224.
12. F. Delime, J. Leger, C. Lamy, *J Appl Electrochem* 29 (1999)1249-1254.
13. C. Coutanceau, S. Brimaud, C. Lamy, J.-M. Leger, L. Dubau, S Rousseau, F Vigier, *Electrochim. Acta* 53 (2008) 6865-6880.
14. A.S. Arico, S. Srinivasan, V. Antonucci, 1 (2001) 133-161.
15. X.H. Xia, H.D. Liess, T. Iwasita, *J. Electroanal. Chem*. 437 (1997) 233-240.
16. R.G. Freitas, M.C. Santos, R.T.S. Oliveira, L.O.S. Bulhões, E.C. Pereira, *J. Power Sources*, 158 (2006) 164-168.
17. S. Song, P. Tsiakaras, *Appl. Catal. B: Environ*. 63 (2006) 187-193.
18. M.K. Jeon, P.J. McGinn*, J. Power Sources* 195 (2010) 2664-2668.
19. W. Li, P. Halder, *Electrochem. Solid State Lett.* 13 (2010) B47-B49.
20. Q. He, S. Mukerjee, *Electrochim. Acta* 55 (2010) 1709-1719.
21. J. Wang, J. Xi, Y. Bai, Y. Shen, J. Sun, L. Chen, W. Zhu, X. Qiu, *J. Power Sources* 164 (2007) 555-560.
22. H.T. Zheng, Y. Li, S. Chen, P.K. Shen*, J. Power Sources* 163 (2006) 371-375.
23. H. Song, X. Qiu, F. Li, *Electrochim. Acta* 53 (2008) 3708-3713.
24. K. Kinoshita, *Carbon: Electrochemical and Physicochemical Properties*, Wiley, New York, 1988, p-319.
25. Z. Chen, X. Qiu , B. Lu , S. Zhang ,W. Zhu, L. Chen, *Electrochem. Commun*. 7 (2005) 593-596.
26. H. Song, X. Qiu, X. Li, F. Li, W. Zhu, L. Chen*, J. Power Sources* 170 (2007) 50-54.
27. L.H. Jiang, G.Q. Sun, Zh.H. Zhou, Sh.G. Sun, Q. Wang, Sh.Y. Yan, H.Q. Li, J. Tian, J.S. Guo, B. Zhou, Q. Xin, *J. Phys. Chem.*B 109 (2005) 8774-8778.
28. L. Cao, F. Scheiba, Ch. Roth, F. Schweiger, C. Cremers, U. Stimming, H. Fuess, L.Q. Chen, W.T. Zhu, X.P. Qiu, *Angew. Chem. Int. Ed*. 45 (2006) 5315-5319.
29. Y.X. Bai, J.J. Wu, J.Y. Xi, J.Sh. Wang, W.T. Zhu, L.Q. Chen, X.P. Qiu, *Electrochem. Commun*. 7 (2005) 1087-1090.
30. T. Ioroi, Z. Siroma, N. Fujiwara, S. Yamazaki, K. Yasuda, *Electrochem. Commun*. 7 (2005) 183-188.
31. H. Chhina, S. Campbell, O. Kesler, *J. Power Sources* 161 (2006) 893-900.

32. G. Korotcenkov, V. Brinzari, A. Cerneavschi, M. Ivanov, V. Golovanov, A. Cornet, J. Morante, A. Cabot, J. Arbiol, *Thin Solid Films* 460 (2004) 315-323.
33. C. Xiangfeng, W. Caihong, J. Dongli, Z. Chenmou, *Chem. Phys. Lett.* 399 (2004) 461-464.
34. N. Iwasa, T. Mayanagi, N. Ogawa, K. Sakata, N. Takezawa, *Catal. Lett.* 54 (1998) 119-123.
35. N. Iwasa, O. Yamamoto, R. Tamura, M. Nishikubo, N.Takezawa, *Catal. Lett*. 62 (1999) 179-184.
36. D. Chu, J. Wang, S. Wang, L. Zha, J. He, Y. Hou, Y. Yan, H. Lin, Z. Tian, *Catal. Commun.* 10 (2009) 955-958.
37. I. S. Park, E. Lee, A. Manthiram, *J. Electrochem. Soc*. 157 (2010) B251.
38. L. Xiao, H. Zhang, E. Scanlon, L.S. Ramanathan, E.W. Choe, D. Rogers, T. Apple, B.C. Benicewicz, *Chem. Mater.* 17 (2005) 5328-5333.
39. J. Mader, L. Xiao, T.J. Schmidt, B.C. Benicewicz, *Adv. Polym. Sci*. 216 (2008) 63-124.
40. J. Lobato, P. Canizares, M.A. Rodrigo, J.J. Linares, *Fuel Cells* 9 (2009) 597-604.

© 2010 by ESG (www.electrochemsci.org)